Nanoscale

Cite this: *Nanoscale*, 2012, **4**, 5998

www.rsc.org/nanoscale

PAPER

Colorimetric photonic hydrogel aptasensor for the screening of heavy metal ions†

Bao-Fen Ye,[ab] Yuan-Jin Zhao,*[ac] Yao Cheng,[a] Ting-Ting Li,[a] Zhuo-Ying Xie,[a] Xiang-Wei Zhao[a] and Zhong-Ze Gu*[ac]

Received 24th June 2012, Accepted 11th August 2012
DOI: 10.1039/c2nr31601c

We have developed a robust method for the visual detection of heavy metal ions (such as Hg^{2+} and Pb^{2+}) by using aptamer-functionalized colloidal photonic crystal hydrogel (CPCH) films. The CPCHs were derived from a colloidal crystal array of monodisperse silica nanoparticles, which were polymerized within the polyacrylamide hydrogel. The heavy metal ion-responsive aptamers were then cross-linked in the hydrogel network. During detection, the specific binding of heavy metal ions and cross-linked single-stranded aptamers in the hydrogel network caused the hydrogel to shrink, which was detected as a corresponding blue shift in the Bragg diffraction peak position of the CPCHs. The shift value could be used to estimate, quantitatively, the amount of the target ion. It was demonstrated that our CPCH aptasensor could screen a wide concentration range of heavy metal ions with high selectivity and reversibility. In addition, these aptasensors could be rehydrated from dried gels for storage and aptamer protection. It is anticipated that our technology may also be used in the screening of a broad range of metal ions in food, drugs and the environment.

Introduction

Heavy metal ions, such as Hg^{2+} and Pb^{2+}, are well-known bioaccumulative, nonbiodegradable and highly toxic pollutants of the environment that pose a risk to human health. The accumulation of heavy metal ions and their conversion to organic compounds in the human body through the food chain can result in a number of severe health problems, such as brain damage, kidney failure and various cognitive and motor disorders.[1] Therefore, routine detection of heavy metal ions is central to the environmental monitoring and safety evaluation of aquatic food supplies. Current techniques for the detection of these ions include atomic absorption spectrometry,[2] X-ray fluorescence spectroscopy[3] and inductively coupled plasma–mass spectrometry (ICP–MS).[4,5] Although these methods can produce ultrasensitive analytical results, they usually require expensive equipment, complicated and time-consuming experiments and high levels of operator skill.

To overcome these limitations, much effort has been devoted to obtaining simple, inexpensive and on-the-spot methods that allow real-time detection of heavy metal ions. Fluorophores[6,7] and chromophores[8,9] have been synthesized as reporters of heavy metal ions. However, only a few of them have high selectivity and most suffer from the limitations of low water solubility, delayed response, irreversibility and/or cross-reactivity with other coexisting metal ions. In contrast, enzyme-based sensors that rely on the inhibition of a catalytic reaction have been used for heavy metal ion detection with improved selectivity.[10,11] However, the enzyme reagent stability, high cost and difficulties associated with enzyme production are often cited as problems in the construction of the sensors. Therefore, it is desirable to develop novel sensors for screening heavy metal ions.

Aptamers are antibody-like single-stranded DNA (or RNA) molecules that can bind to a variety of molecules or ions with high sensitivity and selectivity.[12,13] Due to their inherent advantages of simple production, easy storage, good reproducibility, target versatility, easy modification and convenient regeneration, aptamers are considered to be ideal recognition elements for sensor applications.[14–16] Recent studies have found that Hg^{2+} can specifically interact with thymine bases to form thymine–Hg^{2+}–thymine (T–Hg^{2+}–T) complexes[17] and Pb^{2+} can induce the G-quadruplex structure of ssDNA bases.[18] These findings have inspired the development of several novel sensors for the detection of Hg^{2+} and Pb^{2+} using aptamers as the sensing element.[19–24] However, most of these methods involve complex labeling and/or the need to modify the aptamer with differently labeled

[a]*State Key Laboratory of Bioelectronics, Southeast University, Nanjing, 210096, China. E-mail: gu@seu.edu.cn; yjzhao@seu.edu.cn; Fax: +86 25-83795635; Tel: +86 25-83795635*
[b]*Department of Analytical Chemistry, China Pharmaceutical University, Nanjing, 210009, China*
[c]*Laboratory of Environment and Biosafety Research Institute of Southeast University in Suzhou, Suzhou, 215123, China*

† Electronic supplementary information (ESI) available: SEM images of CPCHs, control experiments, selectivity of the Pb^{2+} aptasensor and diffraction shift of the aptasensor in real water samples. See DOI: 10.1039/c2nr31601c

fluorophores and the signals have to be transduced *via* FRET or colorimetric methods to permit detection. Thus, it is still highly desirable to develop a simple, visual detection method for aptamer-based heavy metal ion analysis.

In this research, we propose a novel aptamer-based sensor to realize the simple and visual detection of heavy metal ions by incorporating the aptamer recognition elements into colloidal photonic crystal hydrogel (CPCH) films. Colloidal crystals, which are assembled from monodisperse nanoparticles, have long been used to construct sensors.[25–29] The periodic variation in the refractive index of the colloidal crystals gives rise to interesting optical properties, such as photonic band gaps (PBGs). Specifically, if these highly ordered colloidal crystals are combined with a stimulus-responsive hydrogel, the hydrogel swelling or shrinking upon the stimulus would lead to a change in the PBGs accompanied by a visually perceptible color change.[30–32] Thus, a key technique for using the colloidal crystal sensor is the stimulus element, which should provide a general method that could work for any specific target. Here, we introduce a target-responsive aptamer into the colloidal crystals and developed the corresponding CPCH aptasensors for the screening of heavy metal ions. When the aptasensors were exposed to a solution of heavy metal ions, the specific binding interaction between the aptamer and its target ions changes the aptamer conformation and triggers shrinkage of the hydrogel. This can be detected as a corresponding blue shift in the Bragg diffraction peak position, which can be used for the quantitative estimation of the amount of target heavy metal ions. Our method performed well in the case of Hg^{2+} and Pb^{2+} analysis. We envision that this colorimetric aptasensor will be a promising candidate for on-the-spot detection of environmentally toxic materials.

Results and discussion

Principle of the aptasensor

The working principle of our aptasensor for heavy metal ion detection is illustrated in Scheme 1. The reversible binding between the aptamer and heavy metal ions as a cross-linking mechanism in a semi-interpenetrating hydrogel network was used to capture the heavy metal ions. Initially, the heavy metal ions were absent and the aptamers adopted a random coil structure. However, when the aptamers were in the heavy metal ion solution, they were able to bind selectively with the heavy metal ions to form an ion–aptamer complex structure, such as a hairpin-like structure, which is observed for the T–Hg^{2+}–T complex (Scheme 1a) and the G-quadruplex structure of the Pb^{2+}–aptamer complex (Scheme 1b). These structural changes of the aptamers are usually not observed and difficult to use directly for metal ion sensing. To solve this problem, we incorporated the aptamer into CPCHs to facilitate the detection of metal ions for the first time (as shown in Scheme 1c). As the specific binding of heavy metal ions and the cross-linked single-stranded aptamers in the CPCHs caused hydrogel shrinkage, this induced a decrease in the lattice spacing of the CPCHs, which was observed as a blue shift of the structural colors or as a corresponding blue shift in the Bragg diffraction peak position. The color change of the CPCHs could be used to estimate, qualitatively, the target ions,

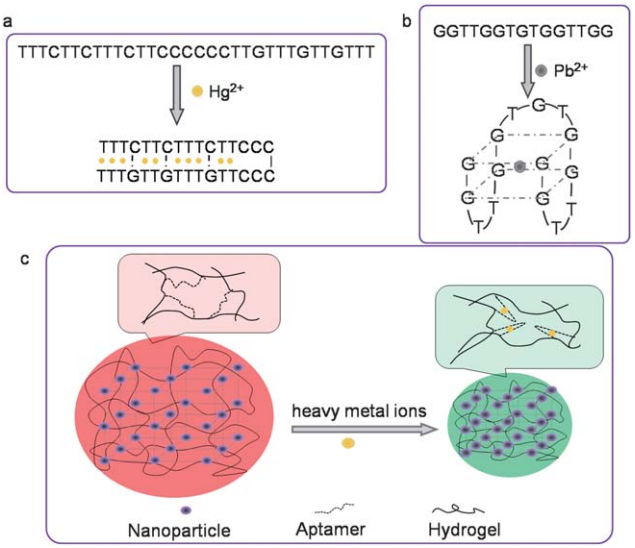

Scheme 1 (a) The aptamer sequence for the detection of Hg^{2+}. (b) The aptamer sequence for the detection of Pb^{2+}. (c) A schematic illustration of the CPCH aptasensor for the detection of heavy metal ions.

while the value of the shift of the Bragg diffraction peak position produced quantitative results regarding the target ions.

In our method, the optical property of the CPCHs is a key point because the sensing process is carried out based on a shift in the diffraction peak. For the high-quality fabrication of the CPCHs, monodisperse silica nanoparticles were thoroughly purified by centrifugation and ion exchange. After these treatments, the highly ordered nanoparticles showed brilliant structural colors and the color of the CPCHs could be controlled by the nanoparticle concentration when the hydrogel component was fixed. The CPCHs, after critical point drying, were characterized by scanning electron microscopy (SEM). As shown in Fig. S1,† a structure with long-range order could be observed and the cross-section SEM image showed hundreds of layers of nanoparticles in the CPCH. In this paper, we prepared CPCHs with a red structural color because the CPCHs undergo a blue shift during detection.

To endow the CPCHs with the ability to screen heavy metal ions, ion-responsive aptamers were incorporated into the

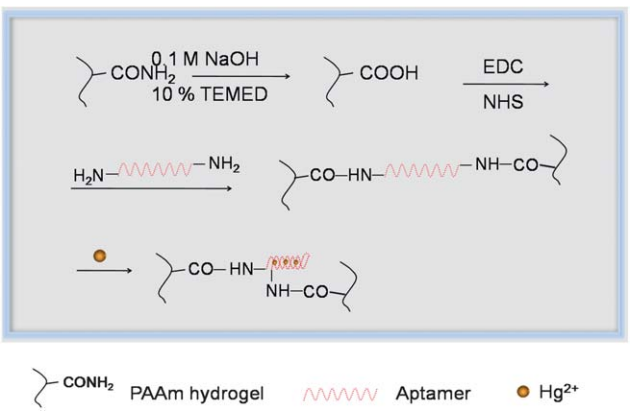

Scheme 2 Preparation of aptamer cross-linked CPCHs for the sensing of heavy metal ions.

CPCHs. As shown in Scheme 2, the CPCHs were first partially hydrolyzed in an NaOH/TEMED solution to convert the amide groups to carboxylates.[31] Because of the carboxylate charge, the hydrolyzed CPCHs swell extensively in PBS. We noticed that the reflection spectrum was undetectable and the structural color disappeared if the hydrolysis time was longer than 90 min. After decreasing the hydrolysis time to 1 h, the hydrolyzed CPCHs exhibited an obvious color and a detectable reflection spectrum. Following this step, 3′- and 5′-amino-modified aptamers were chemically coupled to the hydrogel network of the CPCHs with an EDC/NHS solution, as described in the experimental section. A control experiment with an unhydrolyzed CPCH (as shown in Fig. S2†) proved that only after the hydrolysis procedure can the aptamer be functionalized on the CPCH, which further confirms the formation of the carboxylate groups.

Optimization of the aptasensor

The performance of our aptasensor is strongly influenced by the assay conditions, such as the medium pH, aptamer concentration and binding time. To obtain a higher sensitivity, different assay conditions for the detection of heavy metal ions, such as Hg^{2+} and Pb^{2+}, were investigated.

Take the detection of Hg^{2+} as an example, the binding features of the aptamer were strongly influenced by the buffer pH. The effect of pH on the diffraction shift was studied in NT buffer (20 mM $NaNO_3$, 8 mM Tris nitrate) over the pH range 2.5–9.0. As shown in Fig. 1a, the diffraction shift increased when the pH increased in the range of 4.0–7.0 and the diffraction shift decreased gradually when in the range of 7.5–9.0. At a pH below 7.0, protonation of the nitrogen atoms of the thymine bases reduces its affinity toward Hg^{2+}while at a relatively high pH (>8.0), Hg^{2+} may be complexed by OH^- ions, which, in turn, reduces its ability to complex with the thymine bases.[33] Thus, pH 7.5 buffer was used in subsequent studies.

To investigate the effect of the aptamer concentration on the detection, activated CPCHs were treated with different concentrations of the aptamer solution at room temperature. It was found that the diffraction peak was blue shifted with an increase in the aptamer concentration and this shift reached a plateau at an aptamer concentration of 0.5 mM, as shown in Fig. 1b. Therefore, 0.5 mM aptamer was used in the cross-linking reaction for the aptasensor fabrication.

During the application of our aptasensor, different incubation times also caused a variety of responses. Usually, a long binding time for the aptasensor and Hg^{2+} is expected to yield an enhanced signal, while, for practical use, a shorter assay time is preferred. Therefore, the incubation time was experimentally optimized and the shift in the maximum reflection peak of the aptasensor as a function of time is shown in Fig. 1c. It was found that the shift of the peak increased with the incubation time at short incubation times. After incubation of the aptasensor for 30 min, the peak shift reached a maximum. Further incubation of the sensor did not lead to an obvious peak shift. Thus, we chose an incubation time of 30 min for Hg^{2+} detection in subsequent experiments.

As with the detection of Hg^{2+}, the aptamer–target selectivity recognition performance of Pb^{2+} is also strongly influenced by the binding buffer, aptamer concentration and binding time. Thus, we optimized these parameters to achieve a sensitive assay for Pb^{2+}. It was found that the ideal parameters were pH 7.0 NTN buffer (20 mM $NaNO_3$, 8 mM Tris nitrate, 100 μM NaCN), 0.5 mM Pb^{2+} aptamer for the probe immobilization and 35 min for the capture of Pb^{2+} in the reaction.

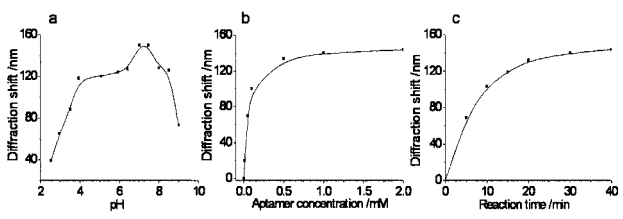

Fig. 1 Optimization of the experimental conditions for Hg^{2+}: (a) pH of the NT buffer; (b) aptamer concentration for the cross-linking; (c) incubation time for the Hg^{2+} binding reaction. (The concentration of Hg^{2+} was 10 mM.)

Analytical performance of the aptasensor

The performance of the aptamer-based assay was assessed with different concentrations of Hg^{2+} under the optimized conditions. In the presence of Hg^{2+}, the aptasensor showed a remarkable volume change (Fig. 2a) and diffraction wavelength shift. It was found that the aptasensor had a diffraction peak at 605 nm and showed a shiny red structural color in the absence of Hg^{2+} (Fig. 2b), while the color and the diffraction peak shifted to blue gradually with an increasing Hg^{2+} concentration. In this process, the color changes were bright and visually evident, as seen in the top photograph in Fig. 2b. Obviously, the diffracted color was easily observed. Thus, our aptasensor could provide a qualitative result for the determination Hg^{2+} levels based on calibration structural color charts.

To investigate further the sensitivity of our method, we analyzed the relationship between the diffraction blue shift and the concentration of Hg^{2+}. Fig. 3a shows the diffraction blue shift of the aptasensor as a function of the mercury concentration. We found that the diffraction shift initially increases with the concentration of Hg^{2+} and becomes saturated at 0.1 mM

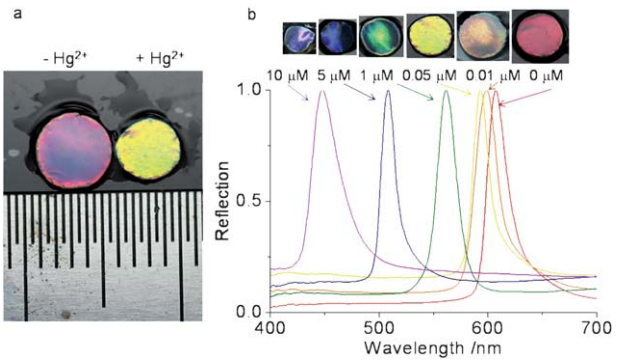

Fig. 2 (a): Volume change of the aptasensor after Hg^{2+} binding. (b): Effect of the Hg^{2+} concentration on the diffraction wavelength of our aptasensor. The diffraction peaks are labeled with the corresponding Hg^{2+} concentration. Top: diffraction color changes from red to blue with an increasing Hg^{2+} concentration.

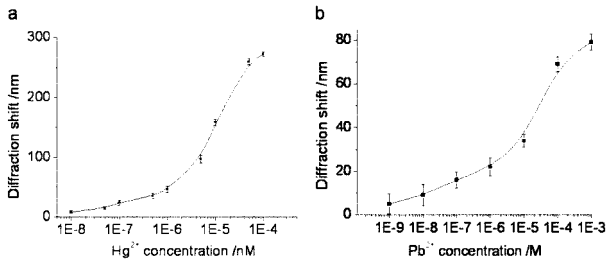

Fig. 3 Diffraction blue shift as a function of the heavy metal ion concentration. (a) Hg^{2+} and (b) Pb^{2+}. Error bars represent the standard deviation of three experiments.

Hg^{2+}. Based on the aptasensor, a relatively wide detection range from 10 nM to 0.1 mM of Hg^{2+} could be achieved. The relative standard deviation (RSD) for three aptasensors to 100 nM Hg^{2+} was 4.2% and the inter-sample variability using one aptasensor to detect different samples was 3.8%. According to the US Environmental Protection Agency (EPA), the toxic level of Hg^{2+} in drinkable water should be below 10 nM. Our proposed Hg^{2+} aptasensor achieves this level of sensitivity. Thus, our research has practical value. In the case of Pb^{2+} screening, our aptasensor showed a large response range toward Pb^{2+} from 1 mM to 1 nM (Fig. 3b).

Selectivity of the aptasensor

A successful sensor should also show high selectivity to its corresponding targets. This is particularly important in the detection of heavy metal ions because of the common coexistence of other heavy metals. Here, the selectivity of our sensor for Hg^{2+} was evaluated by testing the response of the aptasensor to other environmentally relevant metal ions, including Pb^{2+}, Ag^{+}, Mn^{2+}, Zn^{2+}, Mg^{2+}, Ca^{2+}, Al^{3+}, Ba^{2+}, Fe^{3+}, Cu^{2+} and Cr^{3+} at a concentration of 1×10^{-4} M. It was observed that only Hg^{2+} could induce a significant diffraction shift of the aptasensor (Fig. 4). In addition, 1×10^{-6} M Hg^{2+}, in the presence of 100 fold more Pb^{2+} as an interfering ion, was still detected. No significant variations in the diffraction shift were found in comparison with that in the absence of Pb^{2+}. In the case of Pb^{2+} detection, the aptasensor also showed good selectivity against other relevant metal ions (Fig. S3†), which suggested the possibility of the aptasensor's application in real samples.

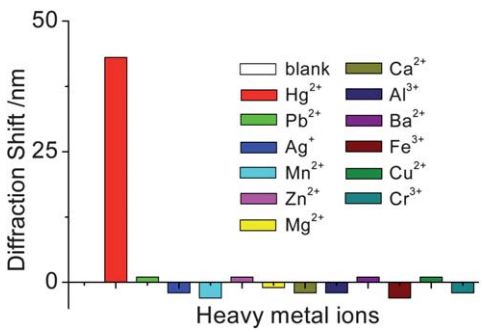

Fig. 4 The effect of various metal ions on the aptasensor diffraction shift. (1 μM for Hg^{2+} and 100 μM each for Pb^{2+}, Ag^{+}, Mn^{2+}, Zn^{2+}, Mg^{2+}, Ca^{2+}, Al^{3+}, Ba^{2+}, Fe^{3+}, Cu^{2+}, and Cr^{3+}).

Regeneration, drying and rehydration of aptasensors

The regeneration procedure of the aptasensor for reuse involves HCl recovery and washing.[21] Following this regeneration procedure, the reflection wavelength returned to its original position, so that the aptasensor could be used with an acceptable reusability and stability (Fig. 5a). The reversible changes of the diffraction peak of the aptasensor with Hg^{2+} are shown in Fig. 5b. The aptasensor showed good durability during tens of cycles and it was found that the change in the diffraction peak was repeatable and reversible.

Drying of the sensor could provide a convenient means for long-term storage, aptamer protection and convenient transportation. During drying, the diffraction peak of the aptasensor shifted to blue and the dry film still showed a bright blue structural colors, which indicated that the ordering of the embedded CCA was maintained during dehydration. After thorough dehydration, we noticed the diffraction of the aptasensors disappeared. Fig. 5c shows the diffraction spectra of the aptasensor during air-drying and rehydration. Diffraction returned within 1 min, indicating that the equilibrium of the resulting aptasensor was achieved within 1 min. The recovered aptasensor retained its mechanical strength and its heavy metal ion sensing ability. The possibility of reversible rehydration of our sensor indicates the potential commercial value that is associated with long-term storage after dehydration.

Verification of the aptasensor performance in water samples

The application of our aptasensors was evaluated through the detection of Hg^{2+} and Pb^{2+} in both tap and lake water samples. For the tap water, the sample was collected after discharging tap water for 30 min, followed by boiling for 5 min to remove chlorine. The lake water sample was from the Xuanwu Lake and was filtered to remove solids before detection. All the water samples were spiked with a known amount of standard Hg^{2+} or Pb^{2+} and then these water samples were diluted with an equal volume of reaction buffer to control the reaction pH. The recovery was investigated by comparing the measured result (Fig. S4†) of Hg^{2+} or Pb^{2+} in the water samples with the added

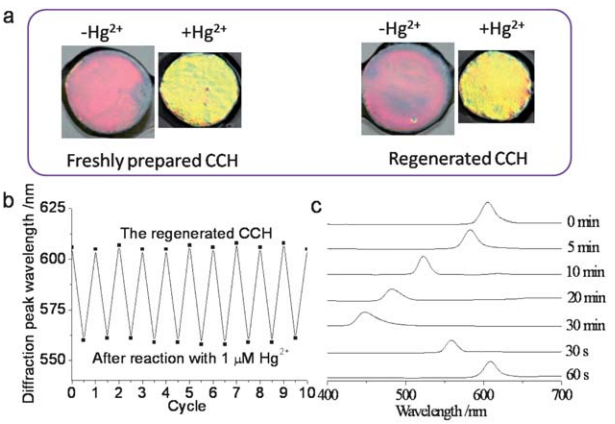

Fig. 5 (a) The response of the freshly prepared aptasensor and the regenerated aptasensor to Hg^{2+}. (b) Reversible changes in the diffraction wavelength of the aptasensor with 1 μM Hg^{2+}. (c) Changes in the diffraction spectra of the aptasensor during air-drying and rehydration.

Table 1 Determination of Hg^{2+} and Pb^{2+} in water samples using the proposed aptasensor

	Amount added (μM)		Amount measured (μM)		Recovery (%)		RSD (%, $n = 3$)	
Sample	Hg^{2+}	Pb^{2+}	Hg^{2+}	Pb^{2+}	Hg^{2+}	Pb^{2+}	Hg^{2+}	Pb^{2+}
Tap water	5.0	5.0	5.1	4.9	102	98	3.7	4.5
Lake water	5.0	5.0	4.8	4.7	96	94	4.2	4.0

value (as summarized in Table 1). It was found that the recovery reached ideal percentages of 94–102%, which suggested that our method was largely free from the matrix effect of real water samples.

Conclusions

In summary, we have successfully combined the advantages of aptamer and colloidal crystals and developed robust aptamer-functionalized CPCHs for the visual detection of heavy metal ions. The CPCHs were derived from a CCA of monodisperse silica nanoparticles, which were polymerized within a polyacrylamide hydrogel. The heavy metal ion-responsive aptamers were cross-linked in the hydrogel network. During the analysis, the specific binding of target heavy metal ions and the cross-linked single-stranded aptamers in the hydrogel network caused hydrogel shrinkage, which was observed as a corresponding blue shift in the Bragg diffraction peak position of the aptasensors. The shift values were used for the quantitative estimation of the amount of target ions. The results showed that our methods could detect a wide concentration range of heavy metal ions, such as Hg^{2+} and Pb^{2+}. The detection limits of both ions satisfactorily met the sensitivity requirements of the US EPA for detecting acceptable levels in drinking water. As detection can be achieved without the aid of sophisticated instrumentation, our technique has the potential to become a generic approach for the monitoring of environmentally toxic materials.

Experimental

Chemicals and materials

The Hg^{2+} aptamer (5′-NH_2–$(CH_2)_6$–TTCTTTCTTCCCCTTGT TTGTT–$(CH_2)_6$–NH_2-3′) and the Pb^{2+} aptamer (5′-NH_2–$(CH_2)_6$–GGTTGGTGTGGTTGG–$(CH_2)_6$–NH_2-3′) were synthesized by Invitrogen Biotechnology Co., Ltd (Shanghai, China) and purified by standard desalting.

N,*N*,*N*′,*N*′-Tetramethylethylenediamine (TEMED), acrylamide (98%, AA), poly(ethylene glycol) diacrylate (PEGDA, M_w 700), *N*,*N*-methylenebisacrylamide (98%, BisAA), lead(II) nitrate and mercury(II) perchlorate were purchased from Alfa Aesar China Ltd. The photoinitiator, 2-hydroxy-2-methylpropiophenone (HMPP), was obtained from Sigma (St Louis, MO) and Irgacure 2959 was from Ciba and used as received. All other metal ion reagents were of analytical reagent grade and were used without further purification or treatment. *N*-(3-Dimethylaminopropyl)-*N*′-ethylcarbodiimide (EDC), *N*-hydroxysuccinimide (NHS), 2-(*N*-morpholino)ethanesulfonic acid (MES) and tris(hydroxymethyl)aminomethane (Tris) were purchased from Aladdin. Milli-Q (Millipore, Bedford, MA) water with ultraviolet (UV) sterilization was used throughout the experiment.

Fabrication of the CPCHs

Monodisperse silica colloidal nanoparticles were synthesized by the Stöber–Fink–Bohn method. The nanoparticles used in this study were 180 nm in diameter. The colloidal nanoparticles were purified *via* centrifugation. The purified colloidal nanoparticles were dispersed in pure water and subsequently shaken with an ion-exchange resin to form a nonclose-packed colloidal crystal array (CCA). After ion exchange, the nanoparticle suspensions became iridescent as a result of Bragg diffraction from the CCA.

The CPCHs were fabricated by free-radical solution photopolymerization using HMPP and Irgacure 2959 as the photoinitiator. In a typical experiment, the pre-gel solution was composed of 10% (v/v) AA/BisAA, 1% (v/v) PEGDA, 1% (v/v) HMPP, 1% Irgacure 2959 and 20% (w/v) of the above CCA solution. After extensive mixing, 10% ion exchange resin (Bio-Rad AG501-X8(D)) was added to the above pre-gel solution. They were shaken together in a small Eppendorf tube until strong diffraction was visually evident, which took about 20 min. The strong structural color of the CPCH indicated the highly ordered array of the monodisperse silica nanoparticles. Then, the pre-gel solution was centrifuged to remove the resin and injected into the polymerization cell, which consisted of two quartz disks separated by 125 μm thick parafilm spacers and exposed to 365 nm UV light (100 W, 10 min) to polymerize the pre-gel solution. The resulting CPCH was rinsed with pure water to remove any unreacted pre-polymer and stored in the hydrated state. Before use, the large-area CPCH film was cut into uniform pieces.

Preparation of aptamer-functionalized CPCHs

First, a small piece of CPCH was hydrolyzed with 10 mL of the aqueous hydrolysis solution containing 0.1 M NaOH and 10% (v/v) TEMED for 1 h to convert amide groups to carboxyl groups. This process exposed many active carboxyl groups in the matrix of the hydrogel. After being washed thoroughly with water, the carboxyl group-functionalized CPCHs were activated with EDC/NHS by immersion in 1 mL pH 6.0 MES buffer solution containing 35 mg EDC and 55 mg NHS for 30 min at room temperature. After activation of the CPCHs, the CPCHs were rinsed several times with pH 6.0 PBS. Then, 2 μL of 0.5 mM aptamer was added and reacted at room temperature for 30 min, followed by refrigeration at 4 °C overnight. After being washed several times with PBS buffer (each soaking for at least 3 h), the aptamer-functionalized CPCHs were obtained through the formation of amide bonds. In the control experiment, the unhydrolyzed CPCH was directly used for aptamer functionalization.

Detection of heavy metal ions

The aptamer-functionalized CPCH was first equilibrated in a reaction buffer (Hg^{2+}: 20 mM $NaNO_3$, 8 mM Tris nitrate, pH 7.5 (NT buffer); Pb^{2+}: 20 mM $NaNO_3$, 8 mM Tris nitrate, 100 μM NaCN, pH 7.0 (NTN buffer)) in a polypropylene tube (diameter:

1.2 cm). To detect Hg^{2+}/Pb^{2+} or other metal ions, different concentrations of Hg^{2+}/Pb^{2+} or 100 μM of the other metal ions were introduced and the aptasensors were incubated in test tubes at 25 °C for 30 min. After extensive washing with the reaction buffer, the reflection spectra of the aptasensors were measured in the reaction buffer at room temperature.

Regeneration of the aptasensors

To regenerate the aptasensors, the hydrogel was soaked in 1 mL of 1% HCl for 3 min. Then, the aptasensors were washed three times with water and twice with reaction buffer (NT buffer for Hg^{2+} aptasensor and NTN buffer for Pb^{2+} aptasensor). The aptasensors were again soaked in 1 mL of 1% HCl. This process was repeated three times. After that, the aptasensors were used for Hg^{2+} or Pb^{2+} detection again.

Drying and rehydration of the hydrogels

To dry the aptamer-functionalized CPCHs, the aptasensors were washed three times with water and then air dried at room temperature for 1 h. For rehydration, the dried aptasensors were directly soaked in the reaction buffer for about 1 min at room temperature. During this process, the reflection spectra were monitored and the water content was determined. The mass of the aptasensor before drying was ~27 mg. After drying, the mass was reduced to ~8 mg. After rehydration, the aptasensor mass recovered to the original value and the reflection spectrum was recovered. The aptasensors were then used for Hg^{2+} or Pb^{2+} detection again.

Detection of Hg^{2+} or Pb^{2+} in tap water and Xuanwu Lake water samples

To evaluate the application of the proposed aptasensors, two types of water samples (tap water and lake water) were collected locally. For tap water, the sample was collected after discharging the tap water for 30 min, followed by boiling for 5 min to remove chlorine. The lake water sample, obtained from Xuanwu Lake, Jiangsu Province, China, was first filtered through a 0.45 μm membrane filter to remove solids. $Hg(ClO_4)_2$ or $Pb(NO_3)_2$ were added to simulate contaminated water. Then, these water samples were diluted with an equal volume of the reaction buffer and analyzed using the proposed method.

Characterization

Photographs of the CPCHs were obtained with a Canon digital camera (EOS 5D Mark II). Reflection spectra of the CPCHs were obtained at a fixed 90° glancing angle utilizing an optical microscope equipped with a fiber-optic spectrometer (Ocean Optics, USB2000-FLG). The microstructures of the CPCHs were characterized by a scanning electron microscope (SEM, Hitachi, S-300N).

Acknowledgements

This research was supported by the National Science Foundation of China (Grant Nos. 50925309, 21105011 and 51073034), the National Science Foundation of Jiangsu (Grant No. BK20122735), the Science and Technology Development Program of Suzhou (Grant No. ZXG2012021), the Scientific Research Foundation of Southeast University (Grant Nos. Seucx201104 and 3207032104) and the 333 Talent Project Foundation. Y. J. Z. also thanks the Postdoctoral Science Foundation of China and Jiangsu province (Grant No. 1201032C).

References

1 I. Onyido, A. R. Norris and E. Buncel, *Chem. Rev.*, 2004, **104**, 5911–5929.
2 O. T. Butler, J. M. Cook, C. F. Harrington, S. J. Hill, J. Rieuwerts and D. L. Miles, *J. Anal. At. Spectrom.*, 2006, **21**, 217–243.
3 S. Arzhantsev, X. Li and J. F. Kauffman, *Anal. Chem.*, 2011, **83**, 1061–1068.
4 J. C. A. De Wuilloud, R. G. Wuilloud, M. F. Silva, R. A. Olsina and L. D. Martinez, *Spectrochim. Acta, Part B*, 2002, **57**, 365–374.
5 Y. F. Li, C. Y. Chen, B. Li, J. Sun, J. X. Wang, Y. X. Gao, Y. L. Zhao and Z. F. Chai, *J. Anal. At. Spectrom.*, 2006, **21**, 94–96.
6 X. F. Guo, X. H. Qian and L. H. Jia, *J. Am. Chem. Soc.*, 2004, **126**, 2272–2273.
7 Y. H. Wang, Y. Q. Huang, B. Li, L. M. Zhang, H. Song, H. Jiang and J. Gao, *RSC Adv.*, 2011, **1**, 1294–1300.
8 M. Suresh, S. K. Mishra, S. Mishra and A. Das, *Chem. Commun.*, 2009, 2496–2498.
9 Nuriman, B. Kuswandi and W. Verboom, *Anal. Chim. Acta*, 2009, **655**, 75–79.
10 C. Chouteau, S. Dzyadevych, C. Durrieu and J. M. Chovelon, *Biosens. Bioelectron.*, 2005, **21**, 273–281.
11 D. Wen, L. Deng, S. J. Guo and S. J. Dong, *Anal. Chem.*, 2011, **83**, 3968–3972.
12 A. D. Ellington and J. W. Szostak, *Nature*, 1990, **346**, 818–822.
13 C. Tuerk and L. Gold, *Science*, 1990, **249**, 505–510.
14 A. B. Iliuk, L. H. Hu and W. A. Tao, *Anal. Chem.*, 2011, **83**, 4440–4452.
15 J. Liu, *Soft Matter*, 2011, **7**, 6757–6767.
16 Z. Zhu, C. Wu, H. Liu, Y. Zou, X. Zhang, H. Kang, C. J. Yang and W. Tan, *Angew. Chem., Int. Ed.*, 2010, **49**, 1052–1056.
17 Y. Miyake, H. Togashi, M. Tashiro, H. Yamaguchi, S. Oda, M. Kudo, Y. Tanaka, Y. Kondo, R. Sawa, T. Fujimoto, T. Machinami and A. Ono, *J. Am. Chem. Soc.*, 2006, **128**, 2172–2173.
18 T. Li, E. Wang and S. Dong, *Anal. Chem.*, 2010, **82**, 1515–1520.
19 A. Ono and H. Togashi, *Angew. Chem., Int. Ed.*, 2004, **43**, 4300–4302.
20 Z. Q. Zhu, Y. Y. Su, J. Li, D. Li, J. Zhang, S. P. Song, Y. Zhao, G. X. Li and C. H. Fan, *Anal. Chem.*, 2009, **81**, 7660–7666.
21 N. Dave, M. Y. Chan, P. J. J. Huang, B. D. Smith and J. W. Liu, *J. Am. Chem. Soc.*, 2010, **132**, 12668–12673.
22 D. Han, S. Y. Lim, B. J. Kim, L. Piao and T. D. Chung, *Chem. Commun.*, 2010, **46**, 5587–5589.
23 L. Wang, T. Li, Y. Du, C. Chen, B. Li, M. Zhou and S. Dong, *Biosens. Bioelectron.*, 2010, **25**, 2622–2626.
24 B. C. Ye and B. C. Yin, *Angew. Chem., Int. Ed.*, 2008, **47**, 8386–8389.
25 M. Kamenjicki, R. Kesavamoorthy and S. A. Asher, *Ionics*, 2004, **10**, 233–236.
26 C. Lopez, *Adv. Mater.*, 2003, **15**, 1679–1704.
27 M. Li, F. He, Q. Liao, J. Liu, L. Xu, L. Jiang, Y. Song, S. Wang and D. Zhu, *Angew. Chem., Int. Ed.*, 2008, **47**, 7258–7262.
28 J. P. Ge, L. He, Y. X. Hu and Y. D. Yin, *Nanoscale*, 2011, **3**, 177–183.
29 S. O. Meade, M. Y. Chen, M. J. Sailor and G. M. Miskelly, *Anal. Chem.*, 2009, **81**, 2618–2625.
30 M. Ben-Moshe, V. L. Alexeev and S. A. Asher, *Anal. Chem.*, 2006, **78**, 5149–5157.
31 D. Arunbabu, A. Sannigrahi and T. Jana, *Soft Matter*, 2011, **7**, 2592–2599.
32 T. Kanai, D. Lee, H. C. Shum, R. K. Shah and D. A. Weitz, *Adv. Mater.*, 2010, **22**, 4998–5002.
33 H. Wang, Y. X. Wang, J. Y. Jin and R. H. Yang, *Anal. Chem.*, 2008, **80**, 9021–9028.